Received: 16 May 2025 | Revised: 28 July 2025 | Accepted: 14 August 2025 | Published online: 27 August 2025

RESEARCH ARTICLE

Remote Sensing for Sustainable Oceans
2025, Vol. 00(00) 1-13
DOI: 10.47852/bonviewRSSO52026174

BON VIEW PUBLISHING

Remotely Observing Dynamics of the Global and Regional Industrial Blue Economies During Macroscale Events

Lyndon E. Llewellyn[1,*]

[1] *Australian Institute of Marine Science, Australia*

Abstract: Ocean-based economic activity, known as the "blue economy", has become increasingly important in recent years to resource managers and government policy-makers. One challenge in understanding the blue economy is tracking how it changes relative to government policies, industry decisions, societal trends, extreme weather events, and environmental catastrophes and better understanding potential links will assist making the blue economy sustainable. Time series analysis can meet this challenge but suitable data is not yet commonplace. Remotely observed marine night light has emerged as a robust proxy for industrial marine economic activity and its repetitive nature, independence, and objectivity can help fill this gap. A previously developed method was modified to create multiple quarterly time series using data collected since 2012 by the Visible Infrared Imaging Radiometer Suite (VIIRS) sensor aboard the Suomi National Polar-orbiting Partnership Satellite. The data comprises absolute night-time radiance measurements after stray light correction. Patterns in marine night light at regional and global scales were analyzed using time series restricted to International Hydrographic Organization (IHO) defined seas and oceans and masking light from land-based sources. Bespoke data extraction code included transformations and analytical settings previously tuned and validated using a time series developed using traditional economic accounting data for Australia and found to also equate to similar data from multiple nations. In this study which used IHO seas to analyze night light data, the global time series for both total and marine-only night light grew over time, except during major events like the 2015 global economic slowdown and the COVID-19 pandemic. Marine and global night light intensities followed parallel trends until the COVID-19 pandemic when marine night light decreased far more sharply than global night light. Until the pandemic, marine night light contributed 2.5–2.7% of global night light, a proportion similar to traditional estimates of the global blue economy scale. Time series from individual seas and oceans varied significantly, likely due to local factors, but cross-correlation pattern analysis revealed correlated changes over time in some geographically connected seas. Combining correlated time series into supra-regional datasets revealed distinct patterns ranging from high volatility in the Indo-Australian Archipelago versus stability in the Middle Eastern seas. Between 2013 and 2024, percentage contributions by different regions to global marine night light changed significantly with the seas of the Indo-Australia Archipelago, Japan, China, South Korea, the Mediterranean, and the Middle East becoming more important. These increases were offset by significant night light declines elsewhere, notably in the North Sea region and the Gulf of Guinea. Being able to remotely sense change over time of industrial marine economic activities at different scales and geographies can enhance blue economic analysis and subsequent policy- and decision-making.

Keywords: blue economy, marine economy, night light, VIIRS, regional, global, marine industry

1. Introduction

Remotely observing the blue economy has emerged in recent years as an independent and subjective method for monitoring economic activity in the marine domain [1–3]. Data from earth observing satellites also allow generation of time series which are not yet common in blue economy research. Time series empower economic analysis through detecting change which might be linked to natural and societal events as well as policy changes or implementation [4]. The existing blue economy time series are usually created by adapting or mining existing economic data that are not specific to marine or ocean sectors and industries [5]. Unlike dedicated efforts such as the recent marine economy satellite account by the US Bureau of Economic Analysis [6] and the European Union Blue Economy Observatory [7], these are not specifically designed for marine or ocean analysis. As an example, in Australia's Index of Marine Industry, marine tourism is calculated by combining data from national statistics and tourism survey data [5]. This scarcity of blue economic time series has prompted efforts to build global capacity in ocean accounting, particularly at the national level [8], which can facilitate international collaboration to better manage blue economies [9]. However, economic accounting can be expensive and requires well developed skills and economic data infrastructure and it is well known that existing economic data is of varied quality throughout the world [10]. In addition, ocean accounting is still maturing as a discipline including how it can be integrated with tools like marine spatial planning to enhance its power [11]. Time series also need to attain a sufficient duration and temporal resolution to become meaningful and useful [12] so initiatives to build economic statistical capability will take some years to yield benefits for many countries. This has prompted recent efforts to explore the utility of satellite data for blue economy research because the data is made freely available, often covers the globe, is uniform, and released frequently [13] with missions sometimes lasting decades. If these efforts are successful, blue economy analysis would benefit as these properties would allow time series construction with an additional benefit of employing a single method to produce global and regional datasets in a consistent and transparent manner.

***Corresponding author:** Lyndon E. Llewellyn, Australian Institute of Marine Science, Australia. Email: L.Llewellyn@aims.gov.au

Night light intensity is a remotely observed parameter that has long been used as a proxy for economic activity [14, 15] although there are limitations in how it can be applied [16]. Restricting night light analysis to the marine domain is also starting to prove fruitful for measuring the marine economy at multiple scales [1, 17]. While night light does not detect all blue economy activity, and usually only that activity that occurs on the sea surface, they capture a substantial portion including offshore oil and gas operations, construction and maintenance of marine infrastructure, shipping and ports, dense fishing activity, offshore aquaculture, and intensity of coastal development; in other words, a large proportion of the industrial component of the blue economy or more simply, the industrial blue economy [18]. Despite night light intensity not capturing all marine economic activity, it has been shown to return measures equivalent to those derived using traditional accounting techniques which can vary for the same nation depending on the organization undertaking the analysis and their preferred method [1]. Consequently, remotely observed night light has the potential to create time series of sufficient resolution to explore changes in marine economic activity attributable to natural events or societal decisions to understand sensitivity and resilience of sectors of the industrial blue economy. To this end, a previous and novel method [1] was modified to increase the temporal resolution from annual to quarterly to create time series from the start of 2013 until the end of 2024. It leveraged data from the Suomi National Polar-orbiting Partnership Satellite which has been delivering data since 2012. This data was accessed through the Google Earth Engine environment and its capability to integrate data within spatially defined regions enabled analysis of the dynamics of night light intensity within individual seas and oceans as defined by the International Hydrographic Organization (IHO) [19]. The resulting database of at-sea economic activity at a regional scale could then be summed to create a global marine night light time series revealing changes at both regional and global scales. This approach to spatial segregation has the advantage of producing data independent of individual national policies and activities although they may influence changes in night light intensity. The resulting database would also allow mining for linkages between regions and any shared responses, or not, to events likely to have regional and world-wide impacts.

Several large-scale events that are quite distinct in nature and known to have impacted global and regional economies have occurred since 2012 [20, 21], the year data from the Visible Infrared Imaging Radiometer Suite (VIIRS) sensor became available. These can prove to be valuable natural experiments [22] for economic analysis at different scales [23]. Time series that capture marine economic activity with adequate temporal resolution and duration, particularly across periods marked by significant disruptive events, offer significant promise for blue economy analysis by capitalizing upon these natural experiments. This study therefore embarked on determining whether time series could be developed and applied to understanding blue economy dynamics and interconnections, and whether natural experiments applied elsewhere in economic analysis could also reveal responsiveness and resilience of marine economies to different types of impactful events.

2. Research Methodology

2.1. Time series creation

Google Earth Engine (GEE) is an open coding environment that allows users to customize remote sensing products. It has previously been used to develop a method for estimating the size of blue economies using night light data from marine regions only [1]. This was achieved by employing masks to exclude night light from land areas when performing calculations within different national jurisdictions. Night light measures offshore oil and gas activities, fishing, aquaculture, shipping including anchorages and associated port activities, and light spill from coastal development, but not daytime activities like many tourism activities. This method was modified here in two ways. Firstly, by restricting data extraction to marine regions by using a set of marine specific shapefiles produced by the International Hydrographic Office, and secondly, recoding so that it calculated the moving 12-month median in quarterly increments since the start of the available data (April, 2012) until December 2024 giving twelve years of quarterly data.

The night light dataset housed in GEE is from the VIIRS (Day/Night Band) on the Suomi Satellite that measures light from around the globe and then filtered by aggregation at the monthly level after excluding light from natural sources. The data is made freely available by the Earth Observation Group, NOAA National Geophysical Data Center [24] in the Google Earth Engine environment. Data processing involves excluding data near the edges of the swath, removing lightning, moon, and cloud-cover effects but not light from aurora, fires, boats, and other temporal lights [25]. Details about the data product and processing can be found at https://eogdata.mines.edu/products/vnl/#monthly. Despite accommodating for cloud-cover in the data processing, data quality may still be affected in those areas that experience extensive and repeated cloud cover during a month [26]. Likewise, despite the VIIRS sensor being superior to its predecessor by having a much larger dynamic range, extremely bright events may saturate the sensor but only for some and not all of the bands [27].

Details for processing this night light data and refining it to measuring marine economies can be found in the original method [1], but in summary:

1) Data for each month was called by the code and scaled to 1000 m^2 pixels.
2) Medians were calculated from the twelve-monthly values from every 12-month period for each pixel as it has been shown that the 12-month median removes high and low radiance outliers [26]. Confidence intervals for the medians were not calculated as it would require a very large number of calculations given the number of pixel medians per analyzed region, development of a bespoke function and access to the raw data. Moreover, the dataset within Google Earth Engine was derived after a number of processing steps including removal of outliers based upon the standard deviation of the original values [25].
3) Noise was reduced by eliminating values <1 so that data could be log10 transformed to remove the influence of occasional extreme light emissions and low values would not be converted into a negative value after log transformation.
4) Light emitted from land-based sources, which may still be contributed from larger islands within sea regions, was removed by masking data using a MODIS derived dataset (MOD44W.006 Terra Land Water Mask Derived from MODIS and SRTM Yearly Global 250 m) [28].
5) Retained data was then summed over the area of interest using shapefiles created as described below.
6) Time series were created by incrementing each calculation by quarter years.

Polygons for each sea were created by subsetting a global shapefile from the International Hydrographic Office [19]. New shapefiles were created for individual seas after extraction and exporting using QGIS (Quantum GIS, version 3.1.4, 2020). It should be noted that, in some instances, this would exclude activities distant from the coast such as within port supply chains which might be included in national blue economy accounts. Nevertheless, the shapefiles for seas and oceans adjacent to land closely traced the coastline, effectively capturing nearly all port, anchorage, and urban nearshore activities. This would result in a slight underestimate that would be minor given the resolution at which this analysis was

undertaken and the focus on global and regional scale trends. These shapefiles were then imported into GEE using the standard GEE protocol. The global time series was constructed by summing all the data for each sea within the IHO dataset. Time series for intermediate regions (e.g., the Mediterranean Sea) were developed by summing all the individual seas (e.g., Adriatic, Aegean, Alboran, and Tyrrhenian Seas plus six others for the Mediterranean). The time series for total global night light (that is marine plus land) was created using the approach above but extracting all night light without any subsetting. The code is located in a Github repository along with a summary of the approach to data extraction and subsequent treatment in the form of a detailed flow chart with a simpler version shown in Figure 1.

Differences between time periods were analyzed on a case-by-case basis to identify areas where changes in night light intensity could influence observed patterns. Differencing is a transformation used with time series to remove the effects of auto-correlation between subsequent data points and is achieved by sequential subtraction of data within a time series. For example, a time series t1, t2, t3, t4 becomes t2 − t1, t3 − t2, and t4 − t3. More detail is provided in the next section and Supplementary Figure S1.

2.2. Trend and pattern analysis

Various packages within the R statistical environment [29] were used to analyze the developed collection of time series for trends and then potential relationships and interdependencies. This included changepoint analysis [30] and determining basic time series properties including how prevalent seasonality was within the developed time series [31] and whether they exhibited linearity, monotonicity or other trends [32].

After this analysis, common or divergent behavior of time series between the different seas and oceans was tested by cross-correlation analysis using the Pearson correlation coefficient (see Supplementary Table S1). Cross-correlation analysis between time series can be confounded if they include seasonal cycles or other trends as correlation requires the two tested variables to be random. The previous analysis therefore served a dual purpose of identifying seasonal cycles or linear trends that would need to be removed to ensure valid cross-correlation analyses. Prior to cross-correlation analysis, time series were differenced by a single lag to make them stationary [33], a prerequisite for making statistically valid correlations between time series, and to eliminate any autocorrelation which may invalidate correlation analysis due to lack of randomness. The value of lagging is exemplified in Supplementary Figure S1a and S1b using two time series from this study. Supplementary Figure S1c demonstrates the results of differencing to remove auto-correlation.

Figure 1

Simplified flow chart describing the logic flow and data handling executed by the code which can be found in a Github repository and a more detailed flowchart

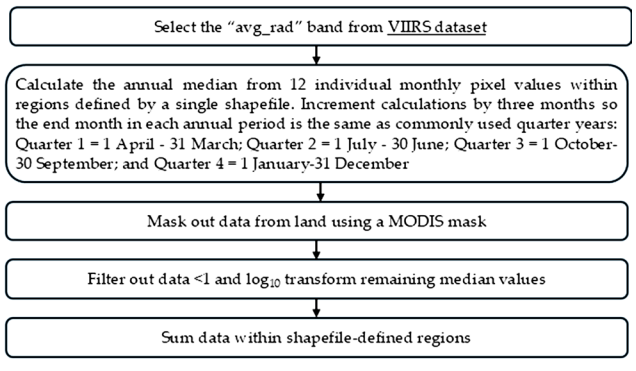

3. Results

3.1. Global scale time series

Time series were generated for every sea within the IHO dataset (n = 105). Aggregating all these time series provides the total amount of night light emitted from the world's marine territories independent of jurisdictional boundaries (Figure 2) which shows changes coincident with global economic events. Both global and marine night light grew from the start of the data series until Q2/Q3 of 2015 (Figure 2a). Likewise, global GDP [34] (Figure 2a inset) grew between 2013 and 2014 before

Figure 2

Patterns within global and marine night light

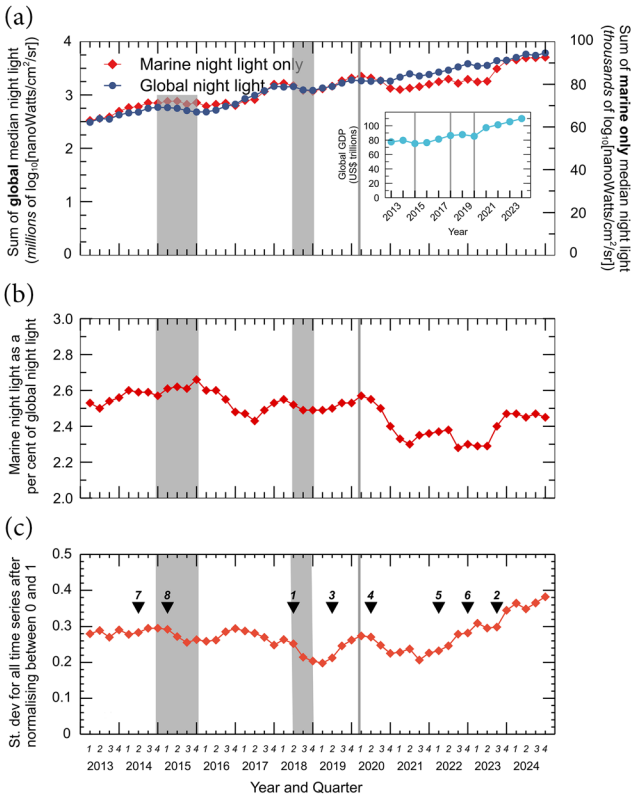

Note: (A) Night light for the globe by quarter (Q) since Q1, 2013 until Q4 of 2023, overlaid with the total night light aggregated from all of the world's oceans as classified by the International Hydrographic Office [19]. The inset in A shows global annual GDP [34]. (B) Marine night light as a proportion of global night light. Night light data in both Panels A and B show data on a quarterly basis with the X-axis depicting the result of summing all of the data for each pixel after annual median values in nanoWatts/cm^2/sr had been log10 transformed. (C) Standard deviation at each time point from the database of time series after they had been normalized to the maximum and minimum for each time series. The arrows indicate the top 8 changepoints detected when using a variance changepoint analysis [38] with the numbers indicating order of appearance as conditions were made less stringent (cpt.var test in R package "changepoint" using the BinSeg method and minimum segment length of 2, and the penalty set manually at 0.05 level and the "normal" test statistic). In all graphs, the grey rectangles and lines depict macroscale events: 1) the year 2015, when a global slowdown occurred [35]; 2) the final quarter of 2018, when economic growth slowed in China and the Euro area [36], and 3) late March, 2020 when COVID-19 was declared a global pandemic by the World Health Organization [37]. For the inset depicting global GDP figures, these lines align with the relevant year.

decreasing in 2015 as a result of a global economic slowdown [35]. Global GDP, marine, and global night light then recommenced growing until a dip in early 2018 for night light, and World Bank GDP figures plateauing between 2018 and 2019. This corresponded with another wide-spread slowing down of economic activity late in 2018, but at a lesser scale than 2015, with China and the Euro region experiencing weakened economic growth married with trade protectionism [36]. The COVID-19 global pandemic was declared in early 2020 [37], dramatically affecting global economic activity, as seen in the World Bank's GDP values, and both marine and global night light decreased at the same time. However, marine night light intensity decreased more significantly relative to global levels during the COVID-19 pandemic than previous decreases. This is further evident from Figure 2b where marine night light as a per cent of global night light dropped from a long-term average of ~2.5% to below 2.3%, returning to near historic levels in late 2023 and plateauing until the end of 2024. This long-term average of ~2.5% prior to 2020 is equal to estimates of the contribution of ocean-based industries to global gross value add in 2010 [38].

Patterns within multiple time series can also be visualized by analyzing variance on a point-wise basis [30]. After normalizing each time series to its minimum and maximum, the standard deviation was calculated for all of the data points from each time series for each time period (Figure 2c). This shows the diversity of the time series decreased at the same times as the global economy experienced shocks due to economic slowdowns in 2015 and 2018 and the onset of the COVID-19 pandemic. However, about 18 months after the pandemic was declared, the standard deviation increased again but went well past historic levels and was continuing to increase at the end of 2024. Most of these changes were also detected using changepoint analysis [39] (Figure 2c), which detects change in both directions.

3.2. Time series for individual seas and oceans

Figure 3 shows the top 10 IHO seas and oceans ranked in order of night light intensity at the start of 2013. These 10 seas comprise 67–72% of global marine night light depending on the year and quarter. The Persian Gulf is the most intense region at the start of 2013 emitting 4–7 times as much night light as the 10th ranked region (Caribbean Sea) at the same times. This is partly due to the difference in size of the region included in the data integration, but this does not completely explain this marked difference as the Persian Gulf is 1/12 the size of the Caribbean Sea. The remaining difference is due to the contrast between the two regions in the intensity, number of locations, and spatial coverage of night light emitting activities. Growth in night light between the top- and bottom-ranked regions in 2013 until 2024 also differed substantially with the amount of night light emitted from the Persian Gulf increasing approximately 50% over these twelve years, keeping it as the most intense region of marine night light in the world, whereas the Caribbean Sea stayed relatively unchanged the whole time period.

Another notable increase in night light intensity was in the South China Sea where it almost doubled between 2013 and 2024 driven by increases along the Vietnamese and southern Chinese coastline, particularly around ports; fishing grounds north-west of Hainan Island; offshore oil and gas producing regions off south Vietnam, and the coastlines of the east Malaysian Peninsula, Sabah, and Sarawak. The Eastern China Sea also doubled in intensity in this time period driven by intensified night light in the Shanghai and Ningbo regions and off the southern coast of the Island of Jeju in South Korea. In contrast, there was a long-term decline in night light in the Gulf of Guinea corresponding with a period of decreasing oil and gas production [40] and increased maritime insecurity [41].

Figure 3
The full time series for the top 10 IHO seas in terms of emitted night light arranged in descending order of intensity in the first quarter of 2013 as are the entries in the legend

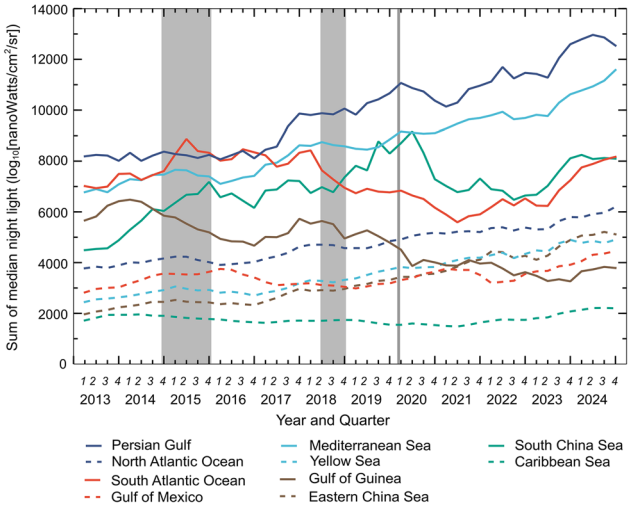

Note: Data for each time series was generated within each sea defined using shapefiles based on the International Hydrographic Organization definitions of the world's seas and oceans with data shown on a quarterly basis with the X-axis depicting the result of summing all of the data for each pixel after calculating annual median values in nanoWatts/cm^2/sr had been log10 transformed.

3.3. Between time series pattern analysis

The potential to up- or downscale analyses using this approach [1] prompted an analysis of whether any of the seas as defined by the IHO behaved in similar manners allowing them to be aggregated into intermediate groupings for regional scale analysis. Correlation analyses between time series can be complicated by high autocorrelation within individual time series (i.e., correlation between a time series and itself when lagged by the chosen time unit). This phenomenon can be seen in Supplementary Figure S1a and S1b which show the autocorrelation between the time series from the Eastern China and Yellow Seas and themselves when lagged by an increasing number of quarters. The effect of differencing on cross-correlation between two time series can also be seen in Supplementary Figure S1c which shows the cross-correlation between the undifferenced and differenced time series for the Eastern China and Yellow Seas. The correlation between the undifferenced time series is very high (nearly 1.0) and remains high and significant for numerous time lags whereas for the differenced time series, the correlation remains high and significant for the unlagged time series only and four quarters later where there was a much smaller but significant negative correlation. Auto-correlation was high and common within all of the time series created for each sea and so differencing was applied to all time series subjected to cross-correlation analysis to make it more statistically robust [42].

Cross-correlation analysis focused upon seas where the average light levels for the whole time series was at least 50 units after summing median values across a region after each pixel (in nanoWatts/cm^2/sr) had been log10 transformed. The selection of this cutoff was based upon the observation that many of the time series below that level were for very small seas and often well below 50, nearing zero and contributing little to the total amount of night light around the world. This resulted in the analysis focusing on the top 43 seas or oceans from the 105 for which time series were initially generated. Prior to differencing for cross-correlation analysis, tests were undertaken for linearity, monotonicity

or other trends and of the 43 subjected to cross-correlation analysis, only a few exhibited statistically significant ($p < 0.05$) trends (details in Supplementary Table S1). Tests for seasonality did not detect any statistically significant ($p < 0.05$) cyclical behavior (data not shown because the test returns a simply true/false Boolean result). Given the absence of seasonality and paucity of trends, detrending or seasonal adjustment was not undertaken prior to pattern analysis because it would be straightforward to determine if any detected correlation would be invalid for those time series affected.

Figure 4 depicts the resulting correlogram for the analyzed seas and oceans and ordered so that they are as geographically near each other as possible. This reveals several groups of high and significant correlations even after differencing. One is the seas within and surrounding the Indo-Australian Archipelago, extending to the South China Sea in the east and the Andaman Sea to the west. Neighboring this region was the Eastern China and Yellow Seas plus the small Seto Naikai which were highly correlated but not with many of the Indo-Australian Archipelago seas. The Sea of Japan was highly correlated to the Seto Naikai but not the Eastern China and Yellow Seas. Given that the Sea of Japan was not correlated to other seas or oceans, it was considered as being able to be grouped with the other three seas. The Philippines Sea was equally correlated to this small grouping and the Indo-Australian Archipelago seas and could be included in either grouping. However, its inclusion in either grouping made no difference

Figure 4
Correlogram showing strength of correlations between time series from IHO defined seas

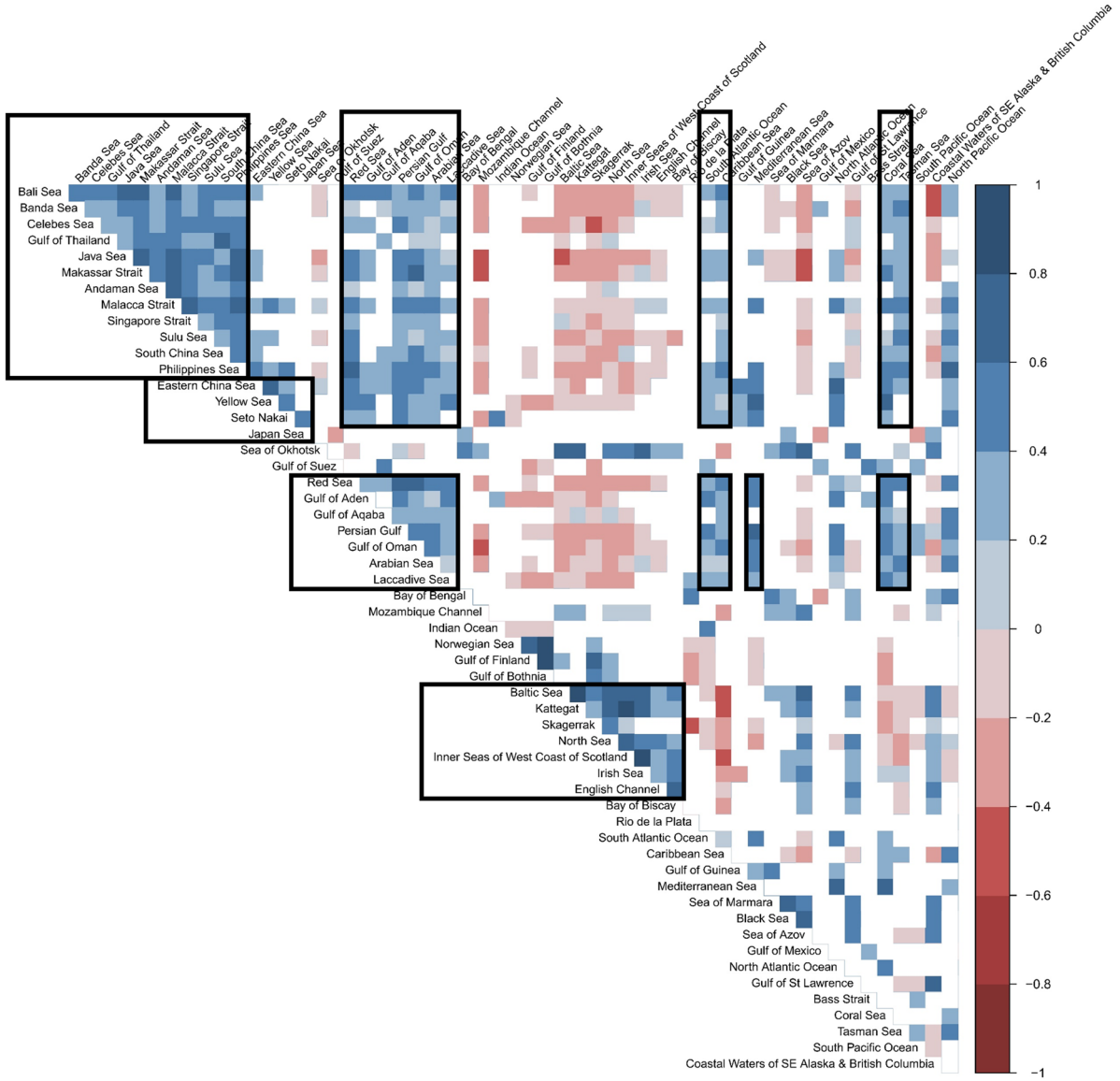

Note: The matrix below depicts the Pearson correlations between IHO seas and oceans, which have been grouped geographically, after quarterly night light intensity time series had been differenced by a single lag. Color indicates a statistically significant correlation ($p < 0.05$) with white meaning no significant correlation. The intensity of the blue and red reflects the strength of the positive or negative correlation, respectively. Only time series where the average for the whole time series for a sea area was greater than 50 after the data for each pixel in a region in nanoWatts/cm^2/sr had been summed across a region and log10 transformed. The rectangles depict some of the groups that are highly positively correlated and geographically near each other. While the Japan Sea was not correlated with the Eastern China and Yellow Seas, it was included with these and the Seto Naikai by virtue of the high positive correlation with the Seto Naikai. The rectangle for the Coral and Tasman Seas also highlights correlations with seas in the Middle East and the Indo-Australian Archipelago.

to the observed aggregated time series of either supra-region like that shown in Figure 5 and described further below, and so was grouped with the seas of the Indo-Australian Archipelago. Another grouping was in the Middle East, dominated by the Persian Gulf but extending to the Red Sea and its connected gulfs (Gulfs of Aqaba and Aden) through the Arabian Sea across to the Laccadive Sea. Smaller groupings were also evident like 1) the North Sea, Kattegat, Skaggerak, Irish Sea and Inner Seas of the West Coast of Scotland, Baltic Sea, English Channel, and Bay of Biscay; 2) the South Atlantic Ocean and Caribbean Sea, and 3) the Tasman and Coral Seas. Correlations between groups geographically distant from each other were also observed such as between the seas of the Middle East and Indo-Australian Archipelago. The Coral and Tasman Seas were highly correlated to each other but also to many seas within the Indo-Australian Archipelago and the Middle East.

3.4. Behavior of regional groupings from cross-correlation analysis

Figure 5 depicts supra-regional time series for the larger groupings detected in Figure 4 by combining data from the above identified groups of seas: the Indo-Australian Archipelago, Middle Eastern region, the North Sea and near neighbors, and finally, the Seto Naikai plus the Eastern China, Yellow, and Japan Seas. Together, these areas emitted 43% of global marine night light in 2013 increasing to 50–51% in 2024. All four regions exhibited markedly different patterns through time with Figure 5 showing the aggregated time series (Figure 5a) highlighted further by depicting the absolute variance of each data point around the mean for each time series in Figure 5b. The Middle East group grew almost continuously apart from plateauing during the 2015 global economic slowdown into 2016 and a year-long dip immediately after the COVID-19 pandemic. Likewise, night light from the Seto Naikai, Eastern China, Yellow, and Japan Seas grouping grew almost linearly between 2013 and 2024 with minor decreases during the 2015 and 2018 economic and trade slowdowns and a brief plateau at the start of the COVID-19 pandemic. In strong contrast, marine night light in the Indo-Australian Archipelago and South China Sea group was highly volatile, dropping markedly after the 2015 global slowdown and an extremely substantial decrease immediately after the COVID-19 global pandemic declaration [37] and did not start to increase in intensity again until mid-2023. Night light from the North Sea region, which included the North Sea, Kattegat, Skaggerak, Irish Sea and Inner Seas of the West Coast of Scotland, Baltic Sea, English Channel, and Bay of Biscay, remained relatively stable and linear apart from some minor decreases coinciding with the 2015 and 2018 global slowdowns. There was no discernible change upon declaration of the COVID-19 pandemic. A minor decrease occurred for a year from mid-2021, followed by a slight recovery and then a gradual and continual decline throughout 2023.

4. Discussion

Night light has often been used as a proxy for economic activity [15, 43] but only recently adapted to marine economic analysis [1, 17]. While the method described in Llewellyn [1], and adapted here, was arrived at using validation with marine economy measures based on traditional accounting methods, the resulting data from total global night (Figure 2a) also mimicked trends within global GDP (Figure 2a inset). Night light continually trended upwards between 2013 and 2024 except for periods when economic activity was impacted at the global scale. This included trade slowdowns at the global scale in 2015 [35] and another in 2018 mostly felt in the Euro region and China [36], and the COVID pandemic in 2020 [37]. Trade slowdowns impact commodity movements around the globe through ports and shipping as well as demand for energy from oil and gas producing regions, both activities whose activity would be reflected in night light intensity.

Figure 5
Patterns in night light intensity over time for supra-regions identified in Figure 4

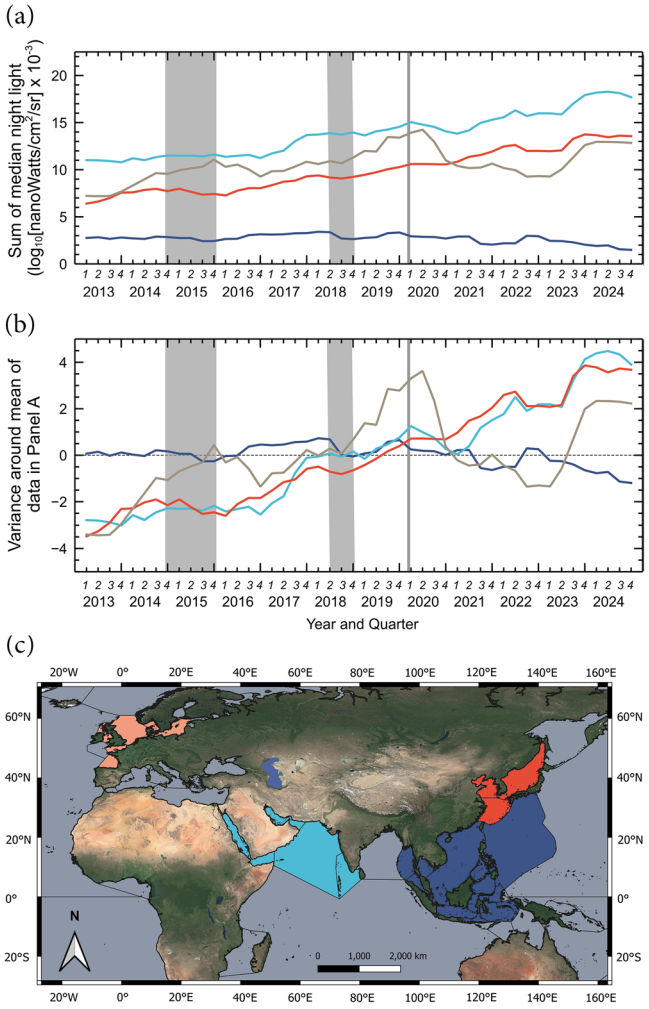

Note: (A) Time series of night light from 2013 Q1 to the end of 2024 for regions comprising: (1) seas of the Indo-Australian Archipelago (Andaman Sea, Bali Sea, Banda Sea, Celebes Sea, Ceram Sea, Flores Sea, Gulf of Boni, Gulf of Thailand, Gulf of Tomini, Java Sea, Makassar Strait, Malacca Strait, Molucca Sea, Philippines Sea, Singapore Strait, South China Sea, and Sulu Sea); (2) Seto Naikai plus the Yellow, Eastern China, and Japan Seas; (3) the Middle East (Persian Gulf, Gulf of Oman, Red Sea, Gulf of Aqaba, Gulf of Aden, and Arabian Sea) plus the Laccadive Sea; and (4) the North Sea and near neighbors (North Sea, Kattegat, Skaggerak, Irish Sea and Inner Seas of the West Coast of Scotland, Baltic Sea, English Channel, and Bay of Biscay). The grey rectangles depict macroscale events the same as in Figure 2. Night light data is shown on a quarterly basis with the X-axis depicting the result of summing all of the data for each pixel after annual median values in nanoWatts/cm^2/sr had been log10 transformed. (B) Data in Panel A transformed into absolute variance around the average for the length of the time series. (C) World map depicting the IHO seas with the supra-regions identified in Figure 4 highlighted using the same colors used for the time series shown in Panel A.

Restricting analysis to just marine night light shows that it contributed between 2.5 and 2.7% of global night light until the first quarter of 2020, when the COVID-19 pandemic was declared [37], after which it trended down, dropping 0.3% as a share of global night

light over the ensuing five quarters before starting to recover and trend upwards (Figure 2b). The decrease in marine night light relative to global night light after the COVID-19 pandemic is far more pronounced than previous global economic events suggesting that different factors were at play during the pandemic within the industrial blue economy relative to the broader global economy. The levels of marine night light prior to the COVID pandemic also closely agrees with estimates of how much the blue economy contributes to the global economy (2.5% [38] and 3.2% [44]). Combining figures for the size of the global economy from the International Monetary Fund [34] and the marine night light percentage values from this study suggests that the global industrial blue economy was at least US$2.0 trillion in 2013, increasing to US$2.7 trillion in 2024 noting that this remote sensing method does not detect all marine industries [1]. The value from 2013 is equivalent to the oft-cited value of at least US$1.5 trillion from 2010 [38], after conversion to 2013 dollars, which was acknowledged as "very conservative" and so likely an underestimate. Likewise, trade in ocean-based goods and services in 2018 was estimated to be worth at least $2.5 trillion per year [45] or "about 3% of global GDP in 2020" [46]. These equivalencies support the use of the marine night light as a proxy for the industrial blue economy.

The point-wise diversity analysis in Figure 2c shows that the responses to the global economic events experienced over the past decade resulted in different responses. Prior to the pandemic, the standard deviation of normalized time series was nearly 0.3, but then decreasing at the same time as the economic slowdowns in 2015 and 2018. After the pandemic was declared, like the previous two events, diversity between time series also reduced but after recovering increased beyond historic levels. More specificity can be obtained regards these changes using changepoint analysis (Figure 2c) enabling exploration of links between policies and other events with changes in marine economic activity demonstrating the value of time series analysis to blue economic analysis as is the case for general economic research [4]. These changes may reflect the vast diversity in policies between nations in terms of how they responded to the pandemic, both at the start and as it started to wane [47]. It remains to be seen whether this increased diversity will remain in the longer term.

Downscaling this analysis to seas and oceans reveals diverse changes in marine night light over time in different locations. Figure 3 shows the top 10 locations in terms of marine light from 2013 to 2024. Night light from most seas and oceans grew over time, apart from fluctuations, some of which coincided with known events. The East Asian seas grew more rapidly than most with the South China, Yellow, and Eastern China Seas essentially doubling between 2013 and 2024 and increasing their combined contribution to global marine night light from 14.4% to 20.4%. The Persian Gulf was the most intense area in terms of marine night light, contributing 11.6% and 14.4% of the globe's marine night light in 2013 and 2024, respectively. This is an area of extensive offshore oil and gas activity, with significant coastal activity in all nations surrounding the Gulf like shipping, ports, and other services that support this sector and catalyzes general coastal development. The Mediterranean Sea is also one of the most intense areas of marine night light and grew since 2013. A highly diversified blue economy, with 22 dependent nations, the region accounts for about 30% of global tourism and 15% of global maritime traffic [48]. Between 2013 and 2024, the total amount of night light grew 53% with growth happening throughout the Mediterranean but more so along the north African coastline. The trajectory for the Mediterranean was also relatively stable, despite changes in global conditions.

Running counter to the growth trajectories was the South Atlantic Ocean and the Gulf of Guinea (Figure 3). Night light intensity within the Gulf of Guinea declined 44% between 2013 and 2024 reducing it from being one of the most luminous seas in 2013 to a mid-tier region. The South Atlantic Ocean is bordered by the south-west coast of Africa, which like the Gulf of Guinea is an area of large-scale off-shore oil and gas extraction and the west coast of South America, dominated by Brazil and Argentina and home to substantial and emerging blue economies built on large coastal cities, commodity ports, and some offshore oil and gas production [49–51]. The North Sea also decreased over this period with light intensity more than halving between 2013 and 2024, albeit with most of that decrease occurring in recent years. The North Sea is experiencing substantial change with the North Sea Transition Authority established to actively manage the diversification of energy production methods as oil and gas production declines and to capitalize on carbon abatement potential within the United Kingdom continental shelf [52].

Accounting for the area covered by the seas within the IHO database, the Singapore Strait is the most intensely lit region per square kilometer (data not shown) followed by the Sea of Marmara and then the Persian Gulf and the Seto Naikai. The Singapore Strait is about 4.5 to 6.6 times more intense than the Persin Gulf depending on the year. Other notable seas within the top 10 based on intensity of light relative to sea surface area were the Gulf of Suez, Rio de la Plata, Gulf of Guinea, and the Yellow Sea. This is unsurprising as these are all areas of intense industrialization and coastal development.

Visual inspection of the numerous time series revealed many similarities but also sufficient differences to prompt pursuit of robust methods of analyzing time series for potential patterns in regional scale behavior of night light intensity. A common pattern analysis strategy is to undertake multiple correlation analyses between pairs of time series after accommodating for any underlying trends which might compromise their statistical validity [42]. After determining that night light time series exhibited no seasonality and the occurrence of trends was minor, pattern analysis was undertaken with those seas containing an average of 50 units after median night light values had been log10 transformed from nanoWatts/cm^2/sr and summed across the sea of interest. All time series were differenced to make them stationary prior to the cross-correlation analysis resulting in the correlogram depicted in Figure 4. The sea regions analyzed were ordered in the correlogram in a manner that maximized geographic proximity. This revealed several aggregations of highly positively correlated time series separated from other groups by low or insignificant correlations (Figure 4). Data from these significantly correlated seas and ocean were combined and further analyzed as "supra-regions" to reveal regional changes of night light intensity in response to macroscale events (Figure 5).

The supra-region containing the North Sea and adjacent seas (Kattegat, Skaggerak, Baltic Sea, Irish Sea, Inner Seas of the West Coast of Scotland, the English Channel, and Bay of Biscay) was relatively stable (Figure 5) and essentially linear except for some minor decreases coinciding with global slowdowns in 2015 and late 2018 and approximately a year after the pandemic, until starting a continuous decline until 2024. The North Sea is the most luminous of the seas within this group and an area of intense, but declining, oil and gas production [53]. However, the North Sea and its neighbors are more than oil and gas and are areas of intense, and multiple uses including growing amounts of offshore renewable energy production [54] and substantial fisheries [55] intermingled with networks of marine protected areas [56]. Oil and gas production is declining in the North Sea itself [53] but numerous industries operate within this and the neighboring seas which are bordered by fifteen nations, highly complicating co-management of environmental and socioeconomic values which are often interdependent [57–59].

Slightly more volatile was the region including the Yellow, Eastern China, and Japan Seas plus Seto Naikai, which grew in a relatively stable manner, with short plateaus in 2015 through to mid-2016 and

again when the COVID-19 pandemic was declared. This region is home to a highly diverse array of marine industrial activity with intense shipping and port activity, fishing, aquaculture, and offshore oil and gas production. It is also home to well over a billion people [60]. It also contains several of the world's megacities, that is urban agglomerations with more than 10 million residents, located on the coast such as Osaka, Seoul, and Shanghai [61]. This stability can be seen elsewhere with cargo throughput of ports like Busan, Incheon, Shanghai, Ningbo, and Tianjin showing almost uninterrupted growth between 2013 and 2023 [62]. It is also an area of strong trade connections [63] and high dependence on the ocean for food [64].

The Middle Eastern Seas group was also relatively stable exhibiting continuous growth from 2013 apart from a decrease at the same time as when the COVID-19 pandemic was declared with growth re-starting a year later (Figure 5a). Industry within the Middle Eastern seas is dominated by offshore oil and gas and onshore industries to support the offshore production. For example, oil and gas production account for 40% of GDP for four of the six Gulf Cooperation Council member countries, added to by construction and transport activity to service this sector [65]. This lack of diversity has been recognized by the nations within this region who are pursuing policies to diversify the industrial blue economies within these areas, particularly away from the oil and gas sector [66, 67]. Saudi Arabia, which has coast-line in both the Red Sea and Persian Gulf appears to have the most ambitious plans for proactive marine economic development and diversification away from oil and gas under their Saudi Arabia 2030 Vision [67]. The oil and gas sector within this region is also unusual in that most of the oil and gas companies operating here are state-owned [68] blurring the lines between the public and private sectors.

In strong contrast, intensity of night light from the seas surrounding the Indo-Australian Archipelago Sea including the South China Sea was highly volatile, dropping markedly after the 2015 global slowdown and severely at the start of the COVID-19 pandemic and remaining low until mid-2023 before increasing in intensity. The collapse of marine night light in 2020 reduced it to levels as low as they were in 2013 and by the end of 2024, had not yet returned to what existed immediately prior to the pandemic. The main drivers of the dramatic changes in the Indo-Australian Archipelago in 2020 were reduced light intensity from:

1) the numerous coastal ports and associated anchorages throughout the region but particularly so for major hubs like Singapore (Figure 6a) and those that service offshore oil and gas fields like Labuan on Sabah Island and Da Nang on the east coast of Vietnam;

Figure 6

Examples of change within seas neighboring Indo-Australian Archipelago nations and near neighbors between immediately prior to the COVID-19 pandemic (Q1, 2020) and the least intense quarter post the pandemic (Q3, 2022)

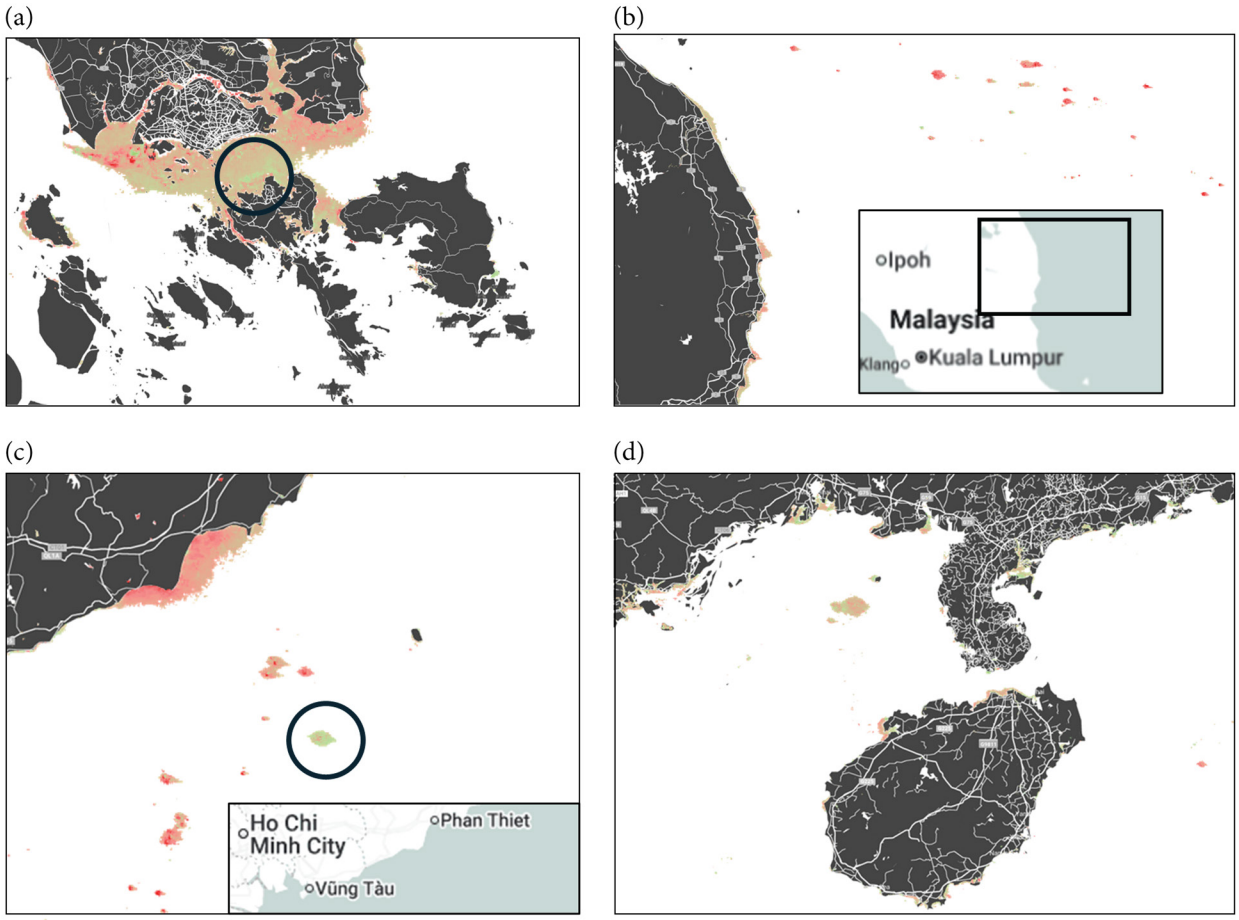

Note: (A) Singapore and surrounding area; (B) off the east coast of the Malaysian Peninsula; (C) the southern coast of Vietnam; and (D) Hainan Island and surrounding area. Panels B and C include insets to highlight the specific locations. Stronger redness indicates a decrease in night light between the two time points and green pixels represent an increase. Circles highlight locations that are examples of activities that run counter to the trend (i.e., intense green whereas the majority of the area is red) and are mentioned in the Discussion. Note that the changes range between −1 and 1 but are dimensionless as they result from differencing between the data generated using this method which is log10 nanoWatts/cm^2/sr).

2) oil and gas fields off the east coast of Malaysia (Figure 6b), southern coast of Vietnam (Figure 6c), and western coasts of Brunei, Sarawak, and Sabah;
3) major offshore fishing grounds northwest of Hainan Island (Figure 6d), throughout the Java Sea and those intermingled with the oil and gas fields mentioned above [69]; and
4) fields of aquaculture farms off southern Vietnam.

However, night light did not universally decrease in these areas as there were some instances where night light increased such as two locations highlighted in panels A and C of Figure 6 which coincided with commissioning of a new oil production platform and an area of intense port activity, respectively. Regarding the latter, reduction in shipping movement can result in an increase in night light emissions as vessels spend more time at anchor in ports, anchorages, or receiving maintenance [17]. As night light intensity recovered during 2023, in the main it was simply a reintensification of night light at the same sites that had experienced a decline.

This supra-region corresponds with one of the few regional, rather than national, blue economy strategies, the Blue Economy Framework produced by the ASEAN nations [70]. The Indo-Australian Archipelago is recognized as one of the world's most important centers of biodiversity [71, 72]. This convergence between volatile industrial marine economic activity and environmental and biodiversity considerations will require sophisticated policies that transcends jurisdictional boundaries, and multiple uses.

While the long-term global trend seen in Figure 2 for marine night light shows that the proportion of global night light from marine sources ranged from 2.3 to 2.7%, depending on global events, the contribution to the total marine night light by different regions has changed over time (Figure 7). The seas surrounding China, Korea, Japan, and the Indo-Australian Archipelago increased from contributing just over 20% of global marine night light at the start of 2013 to almost 30% by the end of 2024. Other areas which showed an increase in this time period was the Mediterranean Sea which increased its global night light contribution by about 2%, and from the Persian Gulf, Red Sea, and neighboring gulfs growing from 17% to almost 20% of global marine night light. Conversely, the contributions from the North Sea and its connecting seas, along with the Gulf of Guinea, more than halved between 2013 and 2024. The total contribution from the seas comprising the Atlantic Ocean decreased several per cent during the same time period. Quah [73] identified a global economic center of gravity in the mid-Atlantic in the 1980s and forecast that it would shift to between India and China by 2050. A similar shift appears to be happening in industrial marine economic activity away from the Atlantic Ocean and neighboring regions to potentially two centers with one in the Indo-Australian Archipelago and East Asia and the other in the Mediterranean and Middle Eastern Seas which are connected by the Suez Canal.

Figure 7
Changes in proportion contribution by different regional groupings of IHO seas

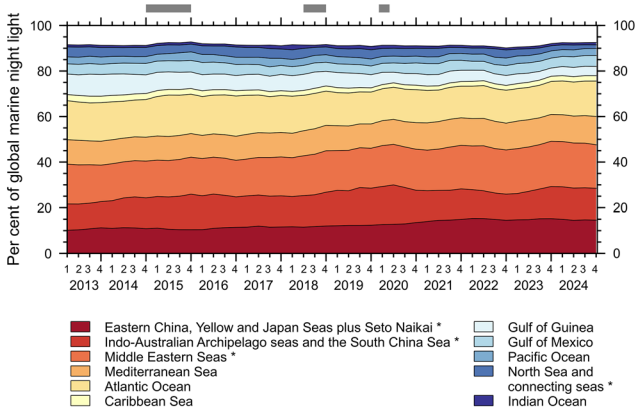

Note: The graph shows the per cent contribution to global marine night light from the four regions shown in Figure 5 (highlighted in the legend with asterisks) and other major seas and oceans (which combine data from several seas) which comprise almost the entirety of marine night light. The grey bars on the top of the graph depict the same global scale economic events shown in Figures 2, 3, and 5.

As noted above, not all industrial marine activity is effectively detected by this method. Emerging industries like marine biotechnology can operate distant from the sea itself and offshore renewable energy may emit little night light. Likewise, sub-sea activity associated with undersea telecommunication cables, seafloor infrastructure for the offshore oil and gas industry, and deep-sea mining will not be quantified. Some, but not all, tourism activity will be detected, specifically activities that occur over multiple days and generate light at nighttime such as accommodation and other offshore infrastructure as well as multi-day ship and boat activities. Development of some of these industries is being actively promoted by multiple countries, growing their contribution to the overall blue economy [74]. The original method was calibrated using a dataset derived from country-based macroeconomic data and only for a single nation, although it was found to provide data similar to that produced using more traditional methods for many countries around the world [1]. There is the potential for the underlying phenomenon to vary between different regions and regionally specific calibrations may be required for more detailed analysis in certain locations, but this is hampered by the availability of appropriate data for such calibrations especially for spatial analyses which are not nation-based and direct information collected about surface-based activities may need to be drawn upon. Despite these limitations, the values derived are equivalent to traditional macroeconomic data and exhibit similar variation in trends caused by large scale events.

5. Conclusion

Global interest in developing the blue economy is rapidly increasing as nations aim to diversify their economies or achieve significant new growth [75]. As a result, policymakers are increasingly focused on identifying effective strategies to support this growth in a sustainable and well-managed way. Economic time series are valuable tools for this purpose, offering insights into trends and potential causal relationships. However, there are currently only a limited number of reliable time series specific to the blue economy due to the challenges of implementing national accounting specific to the ocean.

As an alternative, this study built upon a previously validated method [1] to generate high resolution time series of marine economic activity by tracking changes in night light intensity from 2013 to 2024. The time series were spatially restricted to seas and oceans as defined by the International Hydrographic Office, enabling the identification of regional patterns and the construction of a global time series. These time series overlapped with significant events known to have affected the global economy allowing for detection of varied regional responses. At the global scale, the results aligned with accounting-based estimates of the global ocean economy with marine night light accounting for 2.5–2.7% of global night light until early 2020, when it dropped 0.3% during the COVID-19 pandemic before beginning to recover in 2023.

Cross-correlation analysis revealed clusters of neighboring seas—termed "supra-regions"—that exhibited similar behavior, particularly in response to global events. For instance, Middle Eastern seas showed steady growth throughout the study period, with only a minor dip during the COVID-19 pandemic. In contrast, the Indo-Australian Archipelago displayed high volatility, with repeated declines during global disruptions and a varied delays in the time taken to return to growth. Over the study period, the center of marine economic

activity, as indicated by night light, shifted from the Atlantic to East Asia and the Indo-Australian Archipelago, mirroring broader economic forecasts of a shift toward Asia.

Although emerging sectors within the blue economy may not emit detectable night light, the sectors that do are significant contributors and their dynamics will continue to shape the broader blue economy for years to come. Integrating this data with spatial analysis also enables examination of how different regions respond to the same large-scale events. Ultimately, spatiotemporal analysis using consistent, quality-assured remote sensing data offers a powerful new tool for informed policy and decision-making in the blue economy. As this dataset grows, it will increasingly capture key events and reveal patterns across scales from sub-regional to global. Integration with additional and relevant remote sensing datasets like synthetic aperture radar and Automatic Identification Systems data, as has happened elsewhere [3] will further empower this approach and fill gaps in the economic activity not detected by this method.

Acknowledgement

The author is grateful to Google Inc. for its Earth Engine capability and the various organizations cited within the paper that make their data freely available. The author is also grateful to Dr. Diego Barneche (Australian Institute of Marine Science) for thoughtful comments on the manuscript.

Funding Support

This work was funded by the Australian Institute of Marine Science.

Ethical Statement

This study does not contain any studies with human or animal subjects performed by the author.

Conflicts of Interest

The author declares that he has no conflicts of interest to this work.

Data Availability Statement

The code used is available via Github or transfer within the Google Earth Engine (GEE) environment. Spatial polygons usable in GEE are also available by transfer within GEE (https://earthengine.google.com/).

Author Contribution Statement

Lyndon E. Llewellyn: Conceptualization, Methodology, Software, Formal analysis, Investigation, Resources, Data curation, Writing – original draft, Writing – review & editing, Visualization, Project administration.

References

[1] Llewellyn, L. E. (2022). An open and scalable method for spatial measurement of blue economies. *Frontiers in Marine Science*, *9*, 810498. https://doi.org/10.3389/fmars.2022.810498

[2] Paolo, F. S., Kroodsma, D., Raynor, J., Hochberg, T., Davis, P., Cleary, J., ..., & Halpin, P. (2024). Satellite mapping reveals extensive industrial activity at sea. *Nature*, *625*(7993), 85–91. https://doi.org/10.1038/s41586-023-06825-8

[3] Park, J., Lee, J., Seto, K., Hochberg, T., Wong, B. A., Miller, N. A., ..., & Kroodsma, D. A. (2020). Illuminating dark fishing fleets in North Korea. *Science Advances*, *6*(30), eabb1197. https://doi.org/10.1126/sciadv.abb1197

[4] Stock, J. H., & Watson, M. W. (1988). Variable trends in economic time series. *Journal of Economic Perspectives*, *2*(3), 147–174. https://doi.org/10.1257/jep.2.3.147

[5] Australian Government & Australian Institute of Marine Science. (2023). *The AIMS index of marine industry 2023*. Retrieved from: https://www.aims.gov.au/information-centre/aims-index-marine-industry

[6] Nicolls, W., Franks, C., Gilmore, T., Goulder, R., Mendelsohn, L., Grant, T., ..., & Colgan, C. (2020). *Defining and measuring the U.S. ocean economy*. Bureau of Economic Analysis, US Department of Commerce. Retrieved from: https://search.bea.gov/search?affiliate=u.s.bureauofeconomicanalysis&query=Defining+and+Measuring+the +US+Ocean+Economy+%28PDF%29

[7] European Commission, Directorate-General for Maritime Affairs and Fisheries, Borriello, A., Calvo Santos, A., Feyen, L., Ghiani, M., Guillén, J., McGovern, Petrucco, G., Pistocchi, A., Alonso, M.P., Politiek, H., Quatrini, S., Szymczak, K., Tapoglou, E. (2025) The EU blue economy report 2025, Publications Office of the European Union, Luxembourg. https://data.europa.eu/doi/10.2771/2333701

[8] Fenichel, E. P., Milligan, B., & Porras, I. (2020). *National accounting for the ocean and ocean economy*. World Resources Institute. Retrieved from: https://oceanpanel.org/publication/national-accounting-for-the-ocean-and-ocean-economy/

[9] Loureiro, T. G., Milligan, B., Gacutan, J., Adewumi, I. J., & Findlay, K. (2023). Ocean accounts as an approach to foster, monitor, and report progress towards sustainable development in a changing ocean—The systems and flows model. *Marine Policy*, *154*, 105668. https://doi.org/10.1016/j.marpol.2023.105668

[10] Dang, H.-A. H., Pullinger, J., Serajuddin, U., & Stacy, B. (2023). Statistical performance indicators and index—A new tool to measure country statistical capacity. *Scientific Data*, *10*(1), 146. https://doi.org/10.1038/s41597-023-01971-0

[11] Perkiss, S., McIlgorm, A., Nichols, R., Lewis, A. R., Lal, K. K., & Voyer, M. (2022). Can critical accounting perspectives contribute to the development of ocean accounting and ocean governance? *Marine Policy*, *136*, 104901. https://doi.org/10.1016/j.marpol.2021.104901

[12] Fu, T.-C. (2011). A review on time series data mining. *Engineering Applications of Artificial Intelligence*, *24*(1), 164–181. https://doi.org/10.1016/j.engappai.2010.09.007

[13] Burke, M., Driscoll, A., Lobell, D. B., & Ermon, S. (2021). Using satellite imagery to understand and promote sustainable development. *Science*, *371*(6535), eabe8628. https://doi.org/10.1126/science.abe8628

[14] Henderson, J. V., Storeygard, A., & Weil, D. N. (2012). Measuring economic growth from outer space. *American Economic Review*, *102*(2), 994–1028. https://doi.org/10.1257/aer.102.2.994

[15] Proville, J., Zavala-Araiza, D., & Wagner, G. (2017). Night-time lights: A global, long term look at links to socio-economic trends. *PloS One*, *12*(3), e0174610. https://doi.org/10.1371/journal.pone.0174610

[16] Gibson, J., Alimi, O., & Boe-Gibson, G. (2025). Lost in translation? A critical review of economics research using nighttime lights data. *Remote Sensing*, *17*(7), 1130. https://doi.org/10.3390/rs17071130

[17] Polinov, S., Bookman, R., & Levin, N. (2022). A global assess-

ment of night lights as an indicator for shipping activity in anchorage areas. *Remote Sensing*, *14*(5), 1079. https://doi.org/10.3390/rs14051079

[18] Ahmad, A. U., Jeevan, J., & Ruslan, S. M. M. (2025). Exploring blue economy trends: A study utilizing factorial analysis and thematic analysis. *Journal of Business Sustainability*, *2024*(1), 45–62.

[19] International Hydrographic Organization. (1953). *Limits of oceans and seas* (150-XII-1971). IHO.

[20] McKibbin, W., & Fernando, R. (2023). The global economic impacts of the COVID-19 pandemic. *Economic Modelling*, *129*, 106551. https://doi.org/10.1016/j.econmod.2023.106551

[21] Razzaque, M. A., & Ehsan, S. M. (2019). *Global trade turmoil: Implications for LDCs, small states and Sub-Saharan Africa*. [International Trade Working Paper 2019/03]. https://doi.org/10.14217/af1e7fea-en

[22] Angrist, J. D. (2022). Empirical strategies in economics: Illuminating the path from cause to effect. *Econometrica*, *90*(6), 2509–2539. https://doi.org/10.3982/ECTA20640

[23] Miguel, E., & Mobarak, A. M. (2022). The economics of the COVID-19 pandemic in poor countries. *Annual Review of Economics*, *14*, 253–285. https://doi.org/10.1146/annurev-economics-051520-025412

[24] Earth Observation Group, Payne Institute for Public Policy, & Colorado School of Mines. (2012). *VIIRS Nighttime Day/Night Band Composites Version 1 [Data set]*. Google for Developers. https://developers.google.com/earth-engine/datasets/catalog/NOAA_VIIRS_DNB_MONTHLY_V1_VCMCFG#description (accessed on 22 August, 2021).

[25] Elvidge, C. D., Baugh, K., Zhizhin, M., Hsu, F. C., & Ghosh, T. (2017). VIIRS night-time lights. *International Journal of Remote Sensing*, *38*(21), 5860–5879. https://doi.org/10.1080/01431161.2017.1342050

[26] Elvidge, C. D., Zhizhin, M., Ghosh, T., Hsu, F.-C., & Taneja, J. (2021). Annual time series of global VIIRS nighttime lights derived from monthly averages: 2012 to 2019. *Remote Sensing*, *13*(5), 922. https://doi.org/10.3390/rs13050922

[27] Polivka, T. N., Hyer, E. J., Wang, J., & Peterson, D. A. (2015). First global analysis of saturation artifacts in the VIIRS infrared channels and the effects of sample aggregation. *IEEE Geoscience and Remote Sensing Letters*, *12*(6), 1262–1266. https://doi.org/10.1109/LGRS.2015.2392098

[28] Carroll, M., DiMiceli, C., Wooten, M., Hubbard, A., Sohlberg, R., & Townshend, J. (2017). *MOD44W MODIS/Terra Land Water Mask Derived from MODIS and SRTM L3 Global 250m SIN Grid V006 [Data set]*. NASA EOSDIS Land Processes Distributed Active Archive Center. https://doi.org/10.5067/MODIS/MOD44W.006

[29] Ihaka, R., & Gentleman, R. (1996). R: A language for data analysis and graphics. *Journal of Computational and Graphical Statistics*, *5*(3), 299–314. https://doi.org/10.1080/10618600.1996.10474713

[30] Chen, J., & Gupta, A. K. (2000). *Parametric statistical change point analysis*. USA: Birkhäuser.

[31] Ollech, D. (2021). Seasonal adjustment of daily time series. *Journal of Time Series Econometrics*, *13*(2), 235–264. https://doi.org/10.1515/jtse-2020-0028

[32] Lyubchich, V. (2016). Detecting time series trends and their synchronization in climate data. *Intellect. Innovations. Investments*, (12), 132–137.

[33] Haghbin, H., & Maadooliat, M. (2024). A journey from univariate to multivariate functional time series: A comprehensive review. *WIREs Computational Statistics*, 16(1), e1640. https://doi.org/10.1002/wics.1640

[34] International Monetary Fund. (2024). *World economic outlook database, April 2024*. Retrieved from: https://www.imf.org/en/Publications/WEO/weo-database/2024/April

[35] Georgieva, D., Loayza, N. V., & Mendez-Ramos, F. (2018). *Global trade: Slowdown, factors, and policies*. World Bank Group. Retrieved from: https://documents1.worldbank.org/curated/en/698861520277541852/pdf/Global-trade-slowdown-factors-and-policies.pdf

[36] Santiago, F., Haraguchi, N., & Lavopa, A. (2024). Global trends and world order: Implications for new industrial policies in developing countries. *Journal of Industry, Competition and Trade*, *24*(1), 5. https://doi.org/10.1007/s10842-024-00419-4

[37] Jee, Y. (2020). WHO international health regulations emergency committee for the COVID-19 outbreak. *Epidemiology and Health*, *42*, e2020013.

[38] Organisation for Economic Co-operation and Development. (2016). *The ocean economy in 2030*. Retrieved from: https://www.oecd.org/content/dam/oecd/en/publications/reports/2016/04/the-ocean-economy-in-2030_g1g6439e/9789264251724-en.pdf

[39] Killick, R., Haynes, K., & Eckley I. A. (2024). *changepoint: An R package for changepoint analysis. R package version 2.3*. Retrieved from: https://CRAN.R-project.org/package=changepoint

[40] Augé, B. (2021). *The economic and political consequences of falling oil production in sub-Saharan Africa by 2030*. Retrieved from: https://inis.iaea.org/records/n0cdt-4n921

[41] Agyekum, H. A. (2024). Tackling maritime security in the Gulf of Guinea: Interactions between global shipping and Ghanaian state agents. *African Security*, *17*(1-2), 115–140. https://doi.org/10.1080/19392206.2024.2379186

[42] Yuan, J., & Mills, K. (2005). A cross-correlation-based method for spatial–temporal traffic analysis. *Performance Evaluation*, *61*(2-3), 163–180. https://doi.org/10.1016/j.peva.2004.11.003

[43] Ghosh, T., Powell, R. L., Elvidge, C. D., Baugh, K. E., Sutton, P. C., & Anderson, S. (2010). Shedding light on the global distribution of economic activity. *The Open Geography Journal*, *3*, 147–160. http://dx.doi.org/10.2174/1874923201003010147

[44] Hoegh-Guldberg, O. (2015). *Reviving the ocean economy: The case for action. WWF International*. Retrieved from: https://wwfint.awsassets.panda.org/downloads/reviving_ocean_economy_report_hi_res.pdf

[45] United Nations Conference on Trade and Development. (2021). *Advancing the potential of sustainable ocean-based economies: Trade trends, market drivers and market access*. Retrieved from: https://unctad.org/publication/advancing-potential-sustainable-ocean-based-economies-trade-trends-market-drivers-and

[46] UN Trade and Development. (2022). *5 global actions needed to build a sustainable ocean economy*. Retrieved from: https://unctad.org/news/5-global-actions-needed-build-sustainable-ocean-economy

[47] McKibbin, W., & Fernando, R. (2023). The global economic impacts of the COVID-19 pandemic. *Economic Modelling*, *129*, 106551. https://doi.org/10.1016/j.econmod.2023.106551

[48] Plan Bleu, & UNEP/MAP. (2024). *Unraveling the impact of environmentally harmful subsidies in the Mediterranean: Plan Bleu*. Retrieved from: https://planbleu.org/en/publications/edited-volume-unraveling-the-impact-of-environmentally-harmful-subsidies-in-the-mediterranean/

[49] Carvalho, A. B., & de Moraes, G. I. (2021). The Brazilian

coastal and marine economies: Quantifying and measuring marine economic flow by input-output matrix analysis. *Ocean & Coastal Management*, *213*, 105885. https://doi.org/10.1016/j.ocecoaman.2021.105885

[50] Haddad, E. A., & Araújo, I. F. (2025). Shades of blue: The regional structure of the ocean economy in Brazil. *npj Ocean Sustainability*, *4*(1), 15. https://doi.org/10.1038/s44183-025-00112-x

[51] Morea, J. P. (2023). The economic, social and environmental impacts of offshore oil exploration in Argentina: A critical appraisal. *The Extractive Industries and Society*, *15*, 101295. https://doi.org/10.1016/j.exis.2023.101295

[52] North Sea Transition Authority. (2025). *NSTA Overview 2025*. Retrieved from: https://www.nstauthority.co.uk/about-us/nsta-overview/

[53] Dittmar, M. (2017) A regional oil extraction and consumption model. Part II: Predicting the declines in regional oil consumption. *BioPhysical Economics and Resource Quality*, *2*, 16. https://doi.org/10.1007/s41247-017-0032-1

[54] Glaum, P., Neumann, F., & Brown, T. (2024). Offshore power and hydrogen networks for Europe's North Sea. *Applied Energy*, *369*, 123530. https://doi.org/10.1016/j.apenergy.2024.123530

[55] Dankel, D. J., Skagen, D. W., & Ulltang, Ø. (2008). Fisheries management in practice: Review of 13 commercially important fish stocks. *Reviews in Fish Biology and Fisheries*, *18*(2), 201–233. https://doi.org/10.1007/s11160-007-9068-4

[56] Berkström, C., Wennerström, L., & Bergström, U. (2022). Ecological connectivity of the marine protected area network in the Baltic Sea, Kattegat and Skagerrak: Current knowledge and management needs. *Ambio*, *51*(6), 1485–1503. https://doi.org/10.1007/s13280-021-01684-x

[57] Aschenbrenner, M., & Winder, G. M. (2019). Planning for a sustainable marine future? Marine spatial planning in the German exclusive economic zone of the North Sea. *Applied Geography*, *110*, 102050. https://doi.org/10.1016/j.apgeog.2019.102050

[58] Pinkau, A., & Schiele, K. S. (2021). Strategic Environmental Assessment in marine spatial planning of the North Sea and the Baltic Sea—An implementation tool for an ecosystem-based approach? *Marine Policy*, *130*, 104547. https://doi.org/10.1016/j.marpol.2021.104547

[59] Addamo, A. M., la Notte, A., & Guillen, J. (2024). Status of mapping, assessment and valuation of marine ecosystem services in the European seas. *Ecosystem Services*, *67*, 101631. https://doi.org/10.1016/j.ecoser.2024.101631

[60] Melchiorri, M. (2022). The global human settlement layer sets a new standard for global urban data reporting with the urban centre database. *Frontiers in Environmental Science*, *10*, 1003862. https://doi.org/10.3389/fenvs.2022.1003862

[61] Melchiorri, M., Freire, S., Schiavina, M., Florczyk, A., Corbane, C., Maffenini, L., ..., & Kemper, T. (2024). The multi-temporal and multi-dimensional global urban centre database to delineate and analyse world cities. *Scientific Data*, *11*(1), 82. https://doi.org/10.1038/s41597-023-02691-1

[62] Sahoo, S., & Song, D.-W. (2022). Recent patterns of competition and co-operation among major container ports in Asia: An implication for Busan. *KMI International Journal of Maritime Affairs and Fisheries*, *14*(1), 1–28. https://doi.org/10.54007/ijmaf.2022.14.1.1

[63] Wu, H. (2024). Strategic analysis of the China-Japan-Korea Free Trade Zone. *Advanced Perspectives on Social Sciences and Humanities*, *1*(1), 9–12. http://www.hkasdp.com/index.php/APSSH/article/view/3

[64] Erokhin, V., Tianming, G., & Ivolga, A. (2021). Cross-country potentials and advantages in trade in fish and seafood products in the RCEP member states. *Sustainability*, *13*(7), 3668. https://doi.org/10.3390/su13073668

[65] Kasem, A., & Alawin, M. (2019). Determinants of economic diversification in the GCC countries. *International Review of Social Sciences*, *7*(5), 233–243.

[66] Ahmadipour, Z., & Ahroon, N. (2024). Indian Ocean and blue economy of Persian Gulf Cooperation Council. *The International Journal of Humanities*, *31*(3) 1–22. http://dx.doi.org/10.48311/eijh.31.3.2

[67] Cziesielski, M. J., Duarte, C. M., Aalismail, N., Al-Hafedh, Y., Anton, A., Baalkhuyur, F., ..., & Aranda, M. (2021). Investing in blue natural capital to secure a future for the Red Sea ecosystems. *Frontiers in Marine Science*, *7*, 603722. https://doi.org/10.3389/fmars.2020.603722

[68] Richter, T., & Beck, M. (2021). *Oil and the political economy in the Middle East: Post-2014 adjustment policies of the Arab Gulf and beyond*. UK: Manchester University Press.

[69] Global Fishing Watch. (2025). GFW/Map. Retrieved from: www.globalfishingwatch.org/map/

[70] Meliala, A. (2024). Mapping effective multi regional treaties on blue economy. *Transnational Business Law Journal*, *5*(1), 36–53. https://doi.org/10.23920/transbuslj.v5i1.1609

[71] Tittensor, D. P., Mora, C., Jetz, W., Lotze, H. K., Ricard, D., Berghe, E. V., & Worm, B. (2010). Global patterns and predictors of marine biodiversity across taxa. *Nature*, *466*(7310), 1098–1101. https://doi.org/10.1038/nature09329

[72] Tian, S. Y., Yasuhara, M., Condamine, F. L., Huang, H.-H. M., Fernando, A. G. S., Aguilar, Y. M., ..., & Kase, T. (2024). Cenozoic history of the tropical marine biodiversity hotspot. *Nature*, *632*(8024), 343–349. https://doi.org/10.1038/s41586-024-07617-4

[73] Quah, D. (2011). The global economy's shifting centre of gravity. *Global Policy*, *2*(1), 3–9. https://doi.org/10.1111/j.1758-5899.2010.00066.x

[74] Elston, J., Pinto, H., & Nogueira, C. (2024). Tides of change for a sustainable blue economy: A systematic literature review of innovation in maritime activities. *Sustainability*, *16*(24), 11141. https://doi.org/10.3390/su162411141

[75] Wenhai, L., Cusack, C., Baker, M., Tao, W., Mingbao, C., Paige, K., ..., & Yufeng, Y. (2019). Successful blue economy examples with an emphasis on international perspectives. *Frontiers in Marine Science*, *6*, 261. https://doi.org/10.3389/fmars.2019.00261

[76] Wang, L., & Van Keilegom, I. (2007) Nonparametric test for the form of parametric regression with time series errors. *Statistica Sinica*, *17*, 369-386.

How to Cite: Llewellyn, L. E. (2025). Remotely Observing Dynamics of the Global and Regional Industrial Blue Economies During Macroscale Events. *Remote Sensing for Sustainable Oceans*. https://doi.org/10.47852/bonviewRSSO52026174

Supplementary Figures and Tables

Figure S1
Impact of differencing upon time series autocorrelation and cross-correlation between time series

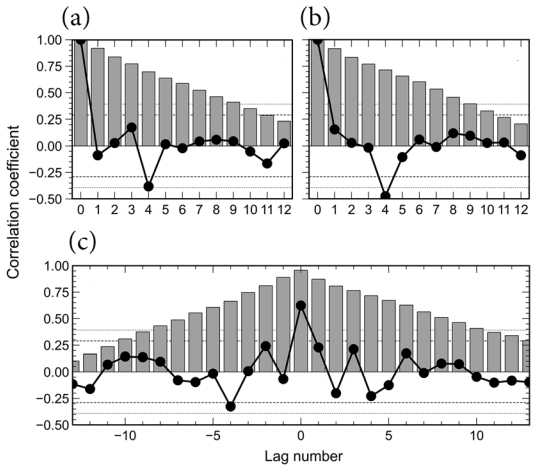

Note: Autocorrelation in the time series for Eastern China (A) and Yellow (B) Seas before (grey bars) and after differencing (black circles) by subtraction of consecutive values at different lags. C) Cross-correlation between the time series for the Eastern China and Yellow Seas before (grey bars) and after differencing of the two time series by a single lag (full black symbols). Panel C shows that the correlation between undifferenced time series was close to 1.0 and time shifting one series against the other incrementally decreases the correlation and remains statistically significant for a substantial number of lags. After the time series have been differenced by a single lag, the correlation between the lagged time series remained over 0.6 and was statistically significant whereas any other correlations were lower and insignificant except for a negative correlation after four lags between the two time series in one direction. In all graphs, the dashed and dotted lines represent the 95% and 99% significance level, respectively.

Table S1
***p* values from trend tests**

IHO Sea Region	Linearity	Monotonicity	Non-monotonic trend
Andaman Sea	0.58	0.89	0.01
Arabian Sea	0.49	0.51	0.75
Baltic Sea	0.25	0.77	0.82
Bay of Bengal	0.61	0.52	0.01
Bay of Biscay	0.08	0.09	0.51
Black Sea	0.72	0.59	0.54
Caribbean Sea	0.26	0.27	0.13
Coral Sea	0.76	0.99	0.03
Eastern China Sea	0.24	0.19	0.36
English Channel	0.08	0.09	0.84
Great Lakes	0.70	0.72	0.15
Gulf of Finland	0.57	0.43	0.72
Gulf of Guinea	0.31	0.43	0.23
Gulf of Oman	0.02	0.22	0.90
Gulf of St Lawrence	0.30	0.20	0.05
Gulf of Suez	0.02	0.02	0.03
Gulf of Thailand	0.86	0.89	0.63
Irish Sea	0.95	0.79	0.93
Java Sea	0.74	0.87	0.63
Laccadive Sea	0.01	0.01	0.01
Malacca Strait	0.95	0.97	0.51
Mozambique Channel	0.66	0.57	0.96
North Sea	0.19	0.41	1.00
Persian Gulf	0.23	0.23	0.97
Philippines Sea	0.95	0.85	0.45
Red Sea	0.63	0.70	0.11
Rio de la Plata	0.90	0.95	0.64
Japan Sea	0.62	0.47	0.31
Sea of Marmara	0.37	0.71	0.82
Seto Naikai	0.79	0.97	0.23
Singapore Strait	0.72	0.82	0.58
South China Sea	0.59	0.81	0.48
Sulu Sea	0.93	0.89	0.02
Tasman Sea	0.76	0.44	0.02
Coastal Waters of SE Alaska & British Columbia	0.07	0.22	0.05
Yellow Sea	0.43	0.29	0.79
Mediterranean Sea	0.69	0.90	0.28
Gulf of Mexico	0.97	0.99	0.30
Indian Ocean	0.79	0.79	0.28
South Atlantic Ocean	0.84	0.98	0.62
North Atlantic Ocean	0.51	0.69	0.61
South Pacific Ocean	1.00	0.91	0.09
North Pacific Ocean	1.00	0.98	0.56

Note: Test were undertaken using the "notrend" test in the "funtimes" package within R [31]. Tests included linearity (Student's *t*-test statistic), monotonicity (Mann–Kendall statistic) or the possibility of a non-monotonic trend [76]. Tests were conducted only on those time series where the average over the whole time series was greater than 100 after the data in nanoWatts/cm^2/sr had been summed across a region and log10 transformed for each pixel within a region. Note that the data for the Mediterranean Sea was a composite of its smaller seas (e.g., Aegean, Alboran etc.). *p* values equal to or less than 0.05 are highlighted.